Numerical investigation of H_2 absorption in an adiabatic high-temperature metal hydride reactor based on thermochemical heat storage: MgH_2 and $Mg(OH)_2$ as reference materials

M. Bhouri[a,*], I. Bürger[b]

[a] Mechanical Engineering, Dalhousie University, B3H 4R2, Halifax, Nova Scotia, Canada

[b] Institute of Engineering Thermodynamics, German Aerospace Center (DLR), D-70569 Stuttgart, Germany

Abstract

A two-dimensional mathematical model to predict the thermal performance of an adiabatic hydrogen storage system based on the combination of magnesium hydride and magnesium hydroxide materials has been developed. A simple geometry consisting of two coaxial cylinders filled with the hydrogen and thermochemical heat storage materials was considered. The main objective was to gain a better knowledge on the thermal interaction between the two storage media, and to determine the dependence of the hydrogen absorption time on the geometric characteristics of the reactor as well as the operation conditions and the thermophysical properties of the selected materials. The dimensions of the two compartments where the two materials are filled were chosen based on the results of a preliminary analytical study in order to compare the absorption times obtained analytically and numerically. The numerical results have shown that the hydrogen absorption process can be completed in a shorter interval of time than analytically as a result of the larger temperature gradient between the magnesium hydride and magnesium hydroxide beds. This was mainly due to variation of temperature in the thermochemical heat storage material during the more realistic dehydration reaction in the numerical solution. Larger temperature gradients, thus a faster hydrogen absorption process can also be achieved by increasing the hydrogen absorption pressure. Moreover, it was found that the increase of the thermal conductivity of the magnesium hydroxide material is crucial for a further improvement of the performance of the MgH_2-$Mg(OH)_2$ combination reactor.

Keywords

Hydrogen storage
Thermochemical heat storage
Magnesium hydride
Magnesium hydroxide
Heat transfer
Numerical study

*Corresponding author. Mechanical Engineering, Dalhousie University, B3H 4R2, Halifax, Nova Scotia, Canada. Tel.: +1 782 234 1368, Fax: +1 902 423 6711.
E-mail address: bhouri_maha@yahoo.fr, maha.bhouri@dal.ca (M. Bhouri)

1. Introduction

With the increasing awareness for economic and environmental concerns related to the use of fossil fuels, and the rising of the global energy demand, there has been an international commitment to make hydrogen the major energy carrier of the future. In this context, several hydrogen and fuel cell research and development programs have been conducted over the last decades [1], targeting first the transportation sector [2,3], and extended thereafter to portable and stationary applications [2,4–6]. Among the encountered technical barriers, the development of a hydrogen storage system with high energy density has been identified as challenging [2]. Such a criterion is closely related to the choice of the hydrogen storage method, as well as the complexity of the hydrogen storage system design [7,8].

In case of large scale stationary applications, magnesium hydride-based hydrogen storage solution has been investigated due to the advantages in terms of energy density, cost, and safety [9–11], with the main focus on improving the energy efficiency of the studied system. Indeed, with an enthalpy of reaction of 75 kJ/mol H_2, a temperature above 300 °C is required to release hydrogen during the endothermic desorption process with an acceptable gravimetric hydrogen storage capacity of about 7 wt. %. Thus, in order to improve the energy efficiency of the system, the heat of reaction which corresponds to up to 31% of the lower heating value of hydrogen has to be exchanged with another system.

Delhomme et al. [10] investigated experimentally the thermal integration of a magnesium hydride (MgH_2) tank with a solid oxide fuel cell (SOFC) stack. In such an integrated system, the waste heat of the SOFC exhaust gases was recovered to provide the energy required for the endothermic desorption process. The heat exchange between the SOFC and the MgH_2 bed was ensured by the mean of a diathermic heat transfer fluid flowing through a finned heat exchanger inserted in the hydrogen storage system. The test of the experimental setup has enabled the identification of technical issues related to the coupling of the SOFC and the MgH_2 tank. Amongst others, it was found that it is necessary to optimize the heat exchanger design and ensure a better thermal insulation in order to achieve higher exchange efficiency between the two coupled systems. In subsequent studies [12,13], the same research group developed an adiabatic hydrogen storage system based on the combination of magnesium hydride and a phase change material (PCM). For such a reactor design, the heat of reaction to be extracted/produced during the hydrogen absorption/desorption processes corresponds to the latent heat of fusion/solidification of the PCM; and heat is conducted from one media to another due to the presence of a temperature gradient between the MgH_2 bed and the PCM. Such an operation principle had directed the choice of the PCM, so that its melting temperature should lay in-between the equilibrium temperatures of absorption and desorption. Besides, special attention was given to ensure that the PCM thermal conductivity does not impact the hydrogen absorption time. Based on these selection criteria, the metallic PCM, $Mg_{69}Zn_{28}Al_3$ with a melting enthalpy of 175 kJ/kg was used for the development of the MgH_2 tank.

Using the same PCM selected by Garrier et al. [13], Mellouli et al. [14] developed a two dimensional mathematical model to compare the performance of cylindrical and spherical configurations of a MgH_2-PCM reactor. Their numerical results showed that a shorter

absorption time is achieved in the case of a spherical configuration, and emphasised the importance of optimizing the amount of used PCM as well as ensuring a perfect insulation of the MgH_2-PCM reactor. The same authors investigated numerically the performance of a Mg_2Ni/Mg_2NiH_4 system where the heat of reaction is stored in a phase change material composed of sodium nitrate, $NaNO_3$ [15,16]. Compared to the basic configuration where the Mg_2Ni alloy occupies the inner part of the tank, and is surrounded by an annular volume filled with the PCM, it was found that a better performance of the hydrogen storage system could be achieved if the PCM is also filled in cylindrical tubes distributed throughout the hydride bed [15], or if the hydrogen storage system is equipped with heat transfer fluid pipes [16].

Although the complexity of the MgH_2 tank was simplified with the use of PCM to store and recover the heat of reaction, the gravimetric capacity of the system was found to be 0.315 wt.% versus 6 wt.% for the MgH_2 + 5 wt.% ENG (expanded natural graphite) pellets incorporated into the storage tank, due to the weight of the PCM [13]. In a recent publication [17], the feasibility of an adiabatic MgH_2 reactor based on thermochemical heat storage has been discussed; and preliminary analytical results have shown that the combination of MgH_2 with magnesium hydroxide ($Mg(OH)_2$) can lead to a competitive hydrogen absorption time compared to the MgH_2-PCM reactor, while reducing the mass of the heat storage media by a factor of 4, using an inexpensive thermochemical heat storage material with a higher energy density compared to the metallic PCM, and operating at more flexible pressure and temperature conditions.

In this new reactor concept, the hydrogen storage media (MgH_2), and the thermochemical heat storage media $Mg(OH)_2$, are filled into two separated compartments of a thermally insulated container. During the uptake of hydrogen, the MgH_2 bed experiences an excessive temperature increase due to the exothermic nature of the H_2 absorption reaction. The released heat of reaction is conducted towards the $Mg(OH)_2$ bed which undergoes an endothermic reaction while storing the same amount of thermal energy, and releasing water vapor to an external water reservoir where the steam is, e.g., condensed. The opposite operation mode of the proposed system consists on the endothermic desorption of H_2. This occurs when the MgH_2 bed absorbs the heat of reaction released by the exothermic hydration reaction of magnesium oxide (MgO). In this case, the water vapor should be externally produced, and then supplied to the thermochemical heat storage media. The two described operating modes are governed by different conditions of temperature and pressure to be imposed to the hydrogen and thermochemical heat storage media as discussed in Ref. [17].

A similar concept has been presented in the case of a portable hydrogen generator patented by Long et al. [18]. The hydrogen generator includes a water supply and an adiabatic system containing a metal hydride (CaH_2), and a chemical hydride ($LiAlH_4$). Through the hydrolysis of CaH_2, hydrogen is generated and the released exothermic reaction heat is transferred to the $LiAlH_4$ media. Once this chemical hydride reaches a temperature above 100 °C, its reaction with the water vapor is initiated as well, and more hydrogen is generated, first through hydrolysis, and then through an endothermic decomposition promoted by the heat that is still available from the exothermic reaction of $LiAlH_4$ with water vapor.

Bürger et al. [19,20] studied an advanced reactor concept for complex hydrides. It is also based on the combination of a low temperature metal hydride ($LaNi_{4.3}Al_{0.4}Mn_{0.3}$) and a high temperature complex hydride (Li-Mg-N-H), separated by a gas permeable layer. The combination reactor, initially at room temperature, is filled with hydrogen at 70 bar. The absorption of hydrogen by the metal hydride is completed in a few seconds at these ranges of temperature and pressure, and its heat of reaction ensures the heat up of the complex hydride bed to a temperature above 130 °C. Accordingly, the absorption of hydrogen by the complex hydride is initiated without the need of an external heat source integration, and a high hydrogen absorption rate is achieved by the Li-Mg-N-H media. Further studies [21,22] based on a one dimensional finite element model and a dimensionless number have been conducted to investigate the dependence of the sorption process on the thicknesses of the two hydrogen storage media, as well as their thermosphysical properties and the operating conditions of the hydrogen storage system.

Despite the similarities between the two systems described in [17–19], the concept of the hydrogen storage reactor based on thermochemical heat storage described here utilizes different hydrogen and heat storage materials, and involves different reactions mechanisms. Besides, there has been no research conducted so far to investigate the H_2 storage process in such a combination reactor. Therefore, as a continuity of the analytical study presented in [17], the aim of this paper is to predict numerically the dynamic performance of the MgH_2-$Mg(OH)_2$ system during the uptake of hydrogen. To this end, a two-dimensional mathematical model describing the kinetics and heat transfer in the two storage media packed in a cylindrical reactor, is first developed. Then, the simulation results are presented to better understand the thermal interaction of both materials; and the resulting H_2 absorption time is compared to the one obtained from the analytical study in order to assess the validity of the assumptions adopted in [17]. Finally, the dependence of the hydrogen storage process on the H_2 absorption pressure and the thermal conductivity of the thermochemical heat storage media is presented and discussed.

2. Model formulation

2.1. Storage media and geometry

Magnesium hydride absorbs hydrogen based on the forward chemical reaction:

$$Mg(s) + H_2(g) \rightleftarrows MgH_2(s) + Q_{abs} \quad (1)$$

Due to the exothermic nature of the hydrogen uptake, the release of the heat of reaction, Q_{abs} results in a sharp increase of the MgH_2 bed temperature. If this temperature reaches the equilibrium temperature corresponding to the H_2 absorption pressure, this would result in the slowdown or the cessation of the absorption reaction [23]. Thus, an efficient cooling of the MgH_2 bed is required.

This is accomplished through the transfer of the heat of reaction, Q_{abs} towards the $Mg(OH)_2$ bed due to the presence of a temperature gradient between the two storage media, as illustrated in Fig.1. As a result, the endothermic dehydration of the $Mg(OH)_2$ material is initiated while storing an amount of heat, Q_{dehy} at temperature and pressure lower than the ones achieved by the MgH_2 bed, based on the forward chemical reaction:

$$Mg(OH)_2\,(s) + Q_{dehy} \rightleftarrows MgO(s) + H_2O(g) \quad (2)$$

and the generated water vapor is released to an external water reservoir where it is condensed or released to the ambient.

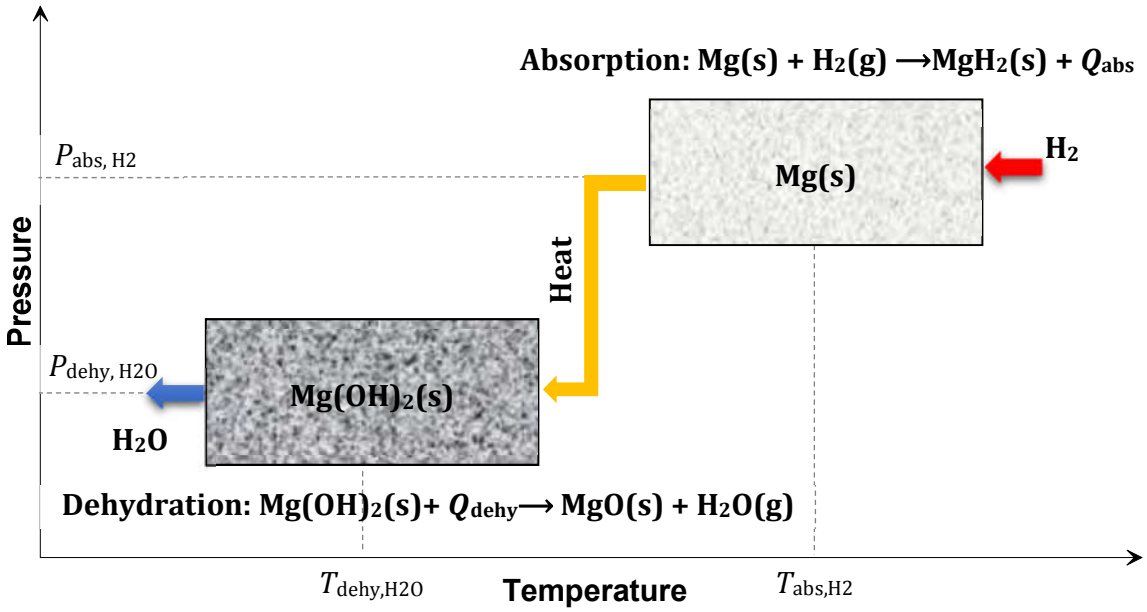

Fig. 1. Operating principle of the MgH_2-$Mg(OH)_2$ combination reactor during the absorption of hydrogen.

Both, magnesium hydride and magnesium hydroxide, suffer from poor thermal conductivities [11], [24,25], which can result in long H_2 absorption and heat storage (Q_{dehy}) times. Studies devoted to the improvement of their thermal properties have shown that the addition of expanded graphite to the powdered form of the two materials, and their compaction into pellets result in a considerable increase of their bulk thermal conductivities, especially in the radial direction [11], [25]. Therefore, in order to take advantage of this thermal characteristic improvement, a cylindrical configuration of the MgH_2-$Mg(OH)_2$ combination reactor is considered in the present study, and it is assumed that the hydrogen and thermochemical heat storage materials are filled into the reactor in a pelletized shape.

The geometry of the combination reactor is illustrated in Fig. 2(a). It consists of two coaxial cylinders, where the MgH_2 and $Mg(OH)_2$ materials are packed into the internal and external compartments of radius R_2 and R_3, respectively. The external cylindrical wall of the reactor is thermally insulated (Radius, R_3), and a filter tube of radius, R_1 is embedded in the centre of the reactor to feed the MgH_2 bed with hydrogen. In order to enable the pressures and temperatures variations during the absorption of hydrogen and the storage of heat, Q_{dehy}, a stainless steel wall separates the two reacting materials. Due to symmetry considerations (45°), the computational domain is taken as one-eighth of the cross section area of the combination reactor as shown in Fig. 2(b).

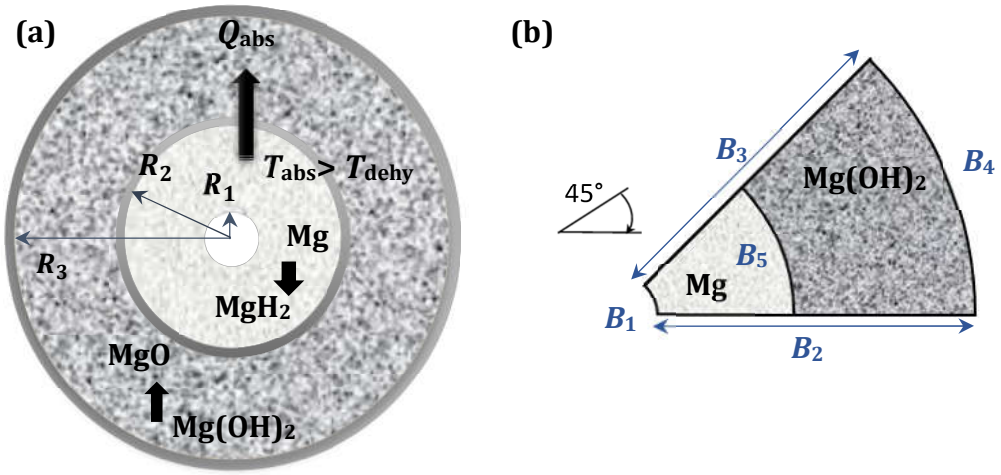

Fig. 2. Geometries of (a) the cross-section of the MgH_2-$Mg(OH)_2$ combination reactor and (b) the one used for computations in the two-dimensional mathematical model.

Even though the studied hydrogen storage system is designated for stationary applications, a reasonable time for the H_2 storage process is always desirable. Based on the results published in [17], it was found that by setting R_2 = 2 cm, and R_1 = 1/4×R_2, a hydrogen absorption time of about 3 hours can be achieved for a $Mg(OH)_2$ bed radius, R_3 of 3.78 cm when the magnesium hydroxide material is completely dehydrated. Therefore, the same values of the MgH_2 and $Mg(OH)_2$ beds radius are used in this study in order to compare the H_2 absorption times issued from the numerical simulation and the analytical analysis.

2.2. Model assumptions

The main assumptions used in the formulation of the mathematical model are as follows:

- There is a local thermal equilibrium between the magnesium hydride and hydrogen, as well as between the magnesium hydroxide and water vapor.
- The influence of the stainless steel layer separating the two storage media on heat transfer is neglected in this first study.
- The hydrogen and water vapor pressures are uniform throughout the magnesium hydride and magnesium hydroxide beds, respectively. Thus, only the kinetics and energy equations of both storage materials are solved.
- Heat transfer by radiation is neglected in both storage media.
- The hydrogen and thermochemical heat storage media do not expand or contract.
- The bed void fractions of the two storage media remain constant and uniform throughout.
- The equation of state of hydrogen is given by the ideal gas law.

2.3. Governing equations

2.3.1. Magnesium hydride bed

The kinetics equations for hydrogen absorption are determined under different conditions of temperature and pressure for compacted disks made of a ball-milling MgH_2 with 5 wt. % of expanded natural graphite, as described in [26,27]:

- $P_{\mathrm{abs}} > 2P_{\mathrm{eq}}$

$$\frac{dx_{\mathrm{abs}}}{dt} = A_{\mathrm{abs}}\exp\left(-\frac{E_{\mathrm{a,abs}}}{\Re T}\right) \cdot \frac{x_{\mathrm{abs}} - 1}{2 \cdot \ln(1 - x_{\mathrm{abs}})} \cdot \left(\frac{P_{\mathrm{abs}}}{P_{\mathrm{eq}}} - 1\right) \quad (3)$$

- $P_{\mathrm{eq}} < P_{\mathrm{abs}} < 2P_{\mathrm{eq}}$

$$\frac{dx_{\mathrm{abs}}}{dt} = A_{\mathrm{abs}}\exp\left(-\frac{E_{\mathrm{a,abs}}}{\Re T}\right) \cdot (1 - x_{\mathrm{abs}}) \cdot \left(\frac{P_{\mathrm{abs}}}{P_{\mathrm{eq}}} - 1\right) \quad (4)$$

The equilibrium pressure, P_{eq} is based on the van't Hoff equation:

$$P_{\mathrm{eq}} = P_0 \cdot \exp\left(\frac{\Delta H_{\mathrm{abs}}}{\Re T} - \frac{\Delta S_{\mathrm{abs}}}{\Re}\right) \quad (5)$$

Referring to the assumptions listed above, the energy equation of the magnesium hydride bed can be written as

$$\left(\rho c_p\right)_{\mathrm{eff}} \frac{\partial T}{\partial t} + \nabla \cdot \left(-\lambda_{\mathrm{MgH_2}} \nabla T\right) = \dot{Q}_{\mathrm{abs}} \quad (6)$$

with

$$\left(\rho c_p\right)_{\mathrm{eff}} = \varepsilon \cdot c_{p,\mathrm{H_2}} \cdot \rho_{\mathrm{H_2}} + (1 - \varepsilon) \cdot c_{p,\mathrm{MgH_2}} \cdot \rho_{\mathrm{MgH_2}} \quad (7)$$

The density of hydrogen is expressed by $\rho_{\mathrm{H_2}} = \frac{P_{\mathrm{abs}} \cdot M_{\mathrm{H_2}}}{\Re \cdot T}$, and the energy source term is given by

$$\dot{Q}_{abs} = (1 - \varepsilon) \cdot \rho_{MgH_2} \cdot w_t \cdot \frac{dx_{abs}}{dt} \cdot \frac{\Delta H_{abs}}{M_{H_2}} \quad (8)$$

2.3.2. Magnesium hydroxide bed

The thermochemical heat storage media used for the modeling of the MgH_2-$Mg(OH)_2$ reactor is a composite material made of $Mg(OH)_2$ and expanded graphite (E.G) with an optimized mixing ratio, $\psi = m_{\mathrm{Mg(OH)_2}}/m_{\mathrm{E.G}}$ of 8, and it is compressed into pellets, called EM8 [28]. Based on the kinetic analysis of the EM8 dehydration into vacuum [29], it was found that the reacted fraction of water vapor can be described by a simple first order model:

$$\frac{dy_{\mathrm{dehy}}}{dt} = -A_{\mathrm{dehy}} \cdot exp\left(-\frac{E_{\mathrm{a,dehy}}}{\Re T}\right) \cdot y_{\mathrm{dehy}} \quad (9)$$

The temporal variation of the density of thermochemical heat storage media is calculated based on the mass equation

$$\frac{\partial \rho_{bed}}{\partial t} = \left(\rho_{\mathrm{Mg(OH)_2}} - \rho_{\mathrm{MgO}}\right) \cdot \frac{dy_{\mathrm{dehy}}}{dt} \quad (10)$$

The energy equations is expressed as

$$\rho_{bed} c_{p,bed} \frac{\partial T}{\partial t} + \nabla \cdot (-\lambda_{bed} \nabla T) = \dot{Q}_{\text{dehy}} \tag{11}$$

where the specific heat capacity, the thermal conductivity, and the energy source term are defined as [30]:

$$c_{p,bed} = \left(\left(1 - y_{\text{dehy}}\right) \cdot c_{p,\text{MgO}} + y_{\text{dehy}} \cdot c_{p,\text{Mg(OH)}_2} \right) \cdot \phi + c_{p,\text{E.G}} \cdot (1 - \phi) \tag{12}$$

$$\lambda_{bed} = \left(1 - y_{\text{dehy}}\right) \cdot \lambda_{\text{MgO}} + y_{\text{dehy}} \cdot \lambda_{\text{Mg(OH)}_2} \tag{13}$$

$$\dot{Q}_{\text{dehy}} = \rho_{\text{Mg(OH)}_2} \cdot \frac{dy_{\text{dehy}}}{dt} \cdot \frac{\Delta H_{\text{dehy}}}{M_{\text{Mg(OH)}_2}} \cdot \phi \tag{14}$$

with ϕ defined as a function of the mixing mass ratio, $\psi = m_{\text{Mg(OH)}_2}/m_{\text{E.G}}$:

$$\phi = \frac{m_{\text{Mg(OH)}_2}}{m_{\text{Mg(OH)}_2} + m_{\text{E.G}}} = \frac{\psi}{\psi + 1} \tag{15}$$

The specific heat capacities of magnesium hydroxide, magnesium oxide, and expanded graphite vary with temperature, and their corresponding functions can be found in [31–33].

The properties of magnesium hydride, hydrogen, and thermochemical heat storage media used in the mathematical model are summarized in Table 1.

Table 1. Input data used in the modeling of MgH_2-$Mg(OH)_2$ reactor [20, 22]

Parameter	Symbol	Value
Magnesium Hydride and Hydrogen		
Enthalpy of absorption reaction (kJ/mol)	ΔH_{abs}	75
Entropy of absorption reaction (kJ/(K.mol))	ΔS_{abs}	135.6
Arrhenius parameter for absorption (1/s)	A_{abs}	10^{10}
Activation energy for absorption (kJ/mol)	$E_{\text{a,abs}}$	130
Material density (kg/m^3)	ρ_{MgH_2}	1,945
Material specific heat capacity (J/(kg.K))	c_{p,MgH_2}	1,545
Thermal conductivity (W/(m.K))	λ_{MgH_2}	10
Porosity (-)	ε	0.44
Gravimetric H_2 storage capacity (wt. %)	w_t	5.94
Hydrogen specific heat capacity (J/(kg.K))	c_{p,H_2}	14,000
Molecular weight of hydrogen (g/mol)	M_{H_2}	2.016

Reference pressure (MPa)	P_0	0.1
Gas constant (J/(mol.K))	$\Re$	8.314
Magnesium Hydroxide		
Enthalpy of dehydration reaction (kJ/mol)	ΔH_{dehy}	81
Arrhenius parameter for dehydration (1/s)	A_{dehy}	13.47×10^{9}
Activation energy for dehydration (kJ/mol)	$E_{\mathrm{a,dehy}}$	157
Magnesium hydroxide density (kg/m^3)	$\rho_{\mathrm{Mg(OH)_2}}$	714
Magnesium oxide density (kg/m^3)	ρ_{MgO}	493.4
Molecular weight of water vapor (g/mol)	$M_{\mathrm{Mg(OH)_2}}$	58.319
Thermal conductivity of $Mg(OH)_2$ (W/(m.K))	$\lambda_{\mathrm{Mg(OH)_2}}$	0.55
Thermal conductivity of MgO (W/(m.K))	λ_{MgO}	0.14
Mixing ratio	ψ	8

2.4. Initial and boundary conditions

Initially, the magnesium hydride bed is at a fully desorbed state ($x_{\mathrm{abs},ini} = 0$), and the magnesium hydroxide bed is at a fully hydrated state ($y_{\mathrm{dehy},ini} = 1$). The two storage media are set at constant temperature and pressure, of 300 °C and 0.1 MPa, respectively. To initiate the hydrogen absorption process, the hydrogen pressure, P_{abs} is exponentially increased with time within the first few minutes to 1 MPa, and then maintained constant throughout the MgH_2 bed.

As described in Section 2.1, the MgH_2-$Mg(OH)_2$ combination reactor is an adiabatic system where heat is only exchanged through the interface between the magnesium hydride and magnesium hydroxide beds. Accordingly, symmetry and thermal insulation boundary conditions are set at the boundaries (B_3 and B_2), and (B_1 and B_4), respectively, as illustrated in Fig. 2(b). At the interface between the hydrogen and thermochemical heat storage media (Boundary B_5 in Fig. 2(b)), the continuity of temperature and heat flux is assumed.

2.5. Numerical procedure

The numerical solution of the two-dimensional model was obtained using the commercial finite element software, COMSOL Multiphysics®, version 5.2a. The magnesium hydride, hydrogen, and magnesium hydroxide properties given in Table 1, along with the aforementioned initial and boundary conditions, were incorporated into the numerical model. A mesh sensitivity analysis has been performed, and a total number of 8439 quadrilateral elements was used.

3. Model validation

Chaise et al. [26], and Zamengo et al. [30] conducted experimental studies to investigate the hydrogen storage process and thermochemical heat storage in magnesium hydride and

magnesium hydroxide tanks, respectively. In order to validate the mathematical model developed for the MgH_2-$Mg(OH)_2$ combination reactor investigated in the current study, the two sets of equations presented above for the MgH_2 and $Mg(OH)_2$ beds were applied to the same experimental hydrogen and thermochemical heat storage tanks geometries described in [26] and [30], with their corresponding initial and boundary conditions, in order to determine the temporal evolutions of the temperature and reacted fractions of hydrogen and water vapor. The comparison of the obtained numerical results and the experimental data is shown in Figs. 3 and 4.

In the case of magnesium hydride tank, the absorption of hydrogen was achieved at initial and set conditions of 300 °C and 0.77 MPa. The temperature was measured at different locations of the MgH_2 bed, and the absorbed volume of H_2 was determined in normal liter (NL), as described in [26]. It can be seen from Fig. 3 that there is a good agreement between the simulation results and the measured temperature profiles at the four selected locations of the MgH_2 bed, especially at the beginning of the hydrogen uptake. With increasing time, the temperature evolution in the simulation is slightly faster than in the experiment, except for the temperature TC1 where a longer simulation time is required to start the cooling of MgH_2 at this location. However, this small effect does not affect the total absorption time which is correctly calculated with the integral value of the absorbed volume.

The dehydration of magnesium hydroxide was experimentally investigated in the case of a cylindrical reactor filled with $Mg(OH)_2$ pellets, and initially at a temperature of 120 °C. A heater was used to maintain the reactor wall at 400 °C, as described in [30]. Comparing the numerical temperature profiles and the dehydrated fraction of water vapor with the ones measured in the case of $Mg(OH)_2$ tank shows that there are some discrepancies, as it can be seen in Fig. 4. Similar observations were reported by Zamengo et al. [30], and the sources of such differences were discussed in the same publication. In our simulation, the dehydration process proceeds at a slightly slower rate than in the experiment; however, it can be assumed that overall, the numerical results describe reasonably the physical phenomena occurring during the thermochemical heat storage, and the mathematical model can be used for the prediction of the thermal behavior of the MgH_2-$Mg(OH)_2$ combination reactor.

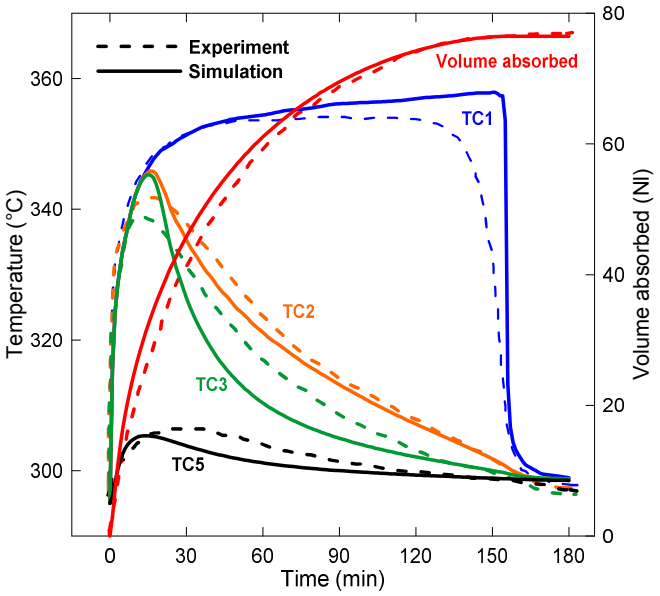

Fig. 3. Comparison of the numerical MgH_2 bed temperature at selected locations and the average H_2 absorbed fraction profiles with experimental data [26] for the validation of the 2D mathematical model of the MgH_2 tank.

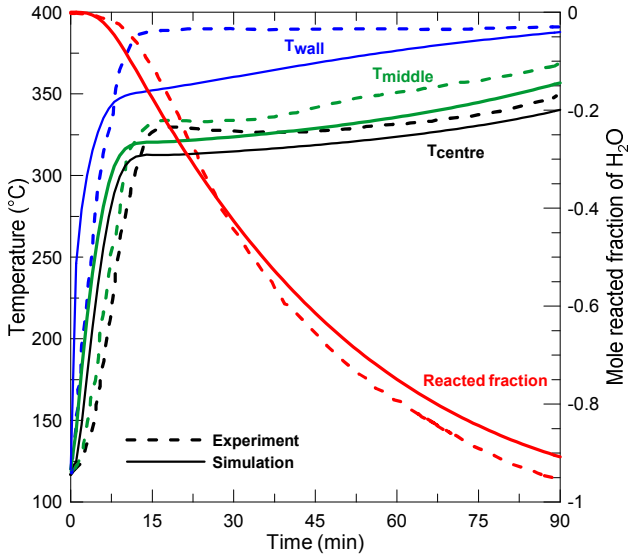

Fig. 4. Comparison of the numerical $Mg(OH)_2$ bed temperature at selected locations and the average H_2O reacted fraction profiles with experimental data [30] for the validation of the 2D mathematical model of the $Mg(OH)_2$ reactor.

4. Results and discussion

4.1. Spatial distributions of the temperature and reacted fractions

The spatial distributions of the temperature and reacted fractions of hydrogen (x_{abs}), and water vapor (y_{dehy}) at selected time intervals are illustrated in Fig. 5(a), (b).

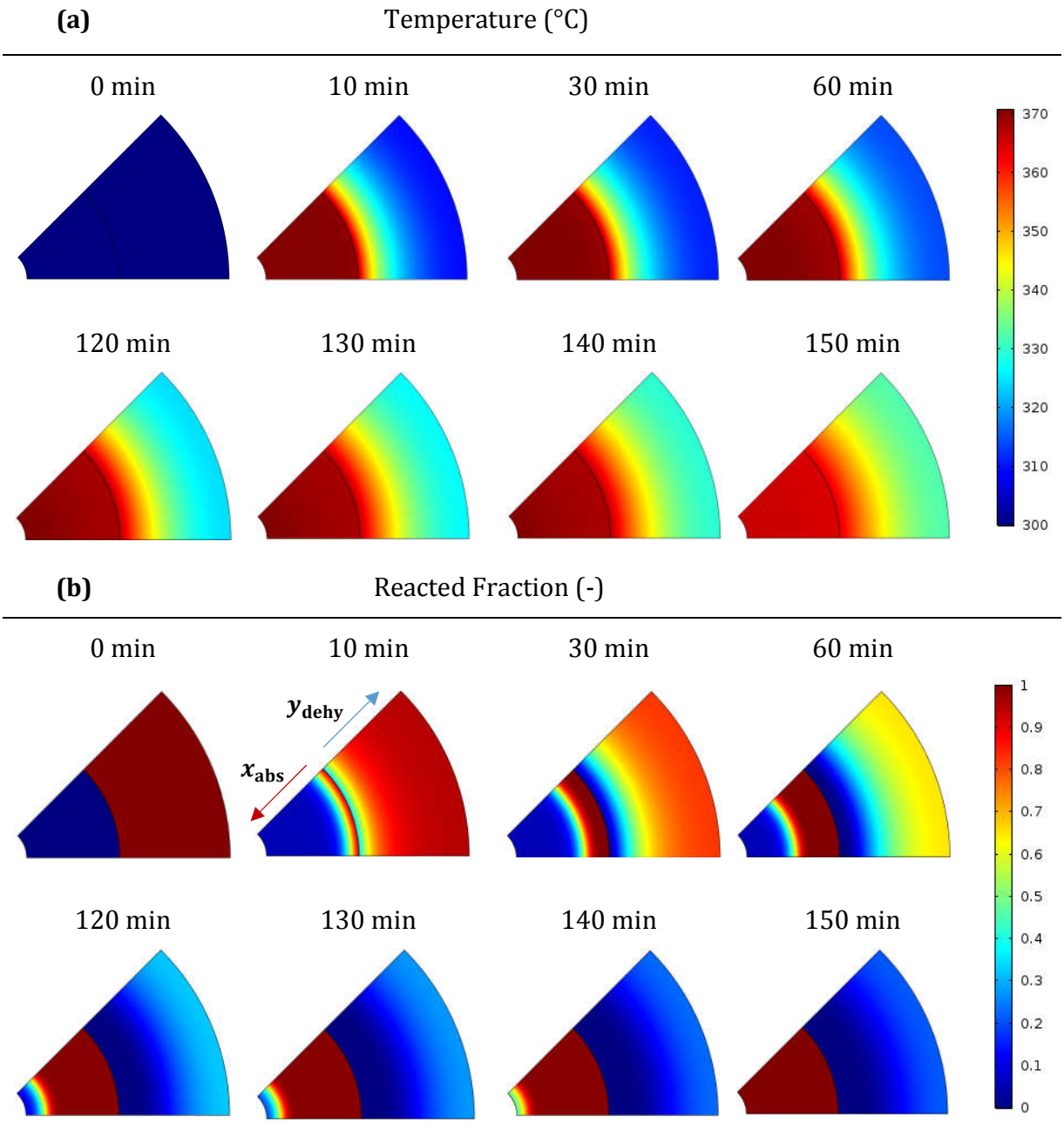

Fig. 5. Spatial distribution of (a) the temperature and (b) the reacted fractions of H_2 and H_2O in the MgH_2-$Mg(OH)_2$ combination reactor at selected times. (The red and blue arrows show the direction of motion of the H_2 absorption front and the dehydration front, respectively).

As described earlier, the hydrogen uptake in the MgH_2 bed is initiated by the increase of the H_2 pressure from 0.1 MPa to 1 MPa. Due to the exothermic nature of the hydrogen absorption reaction, a sharp increase of the MgH_2 bed temperature from 300 °C (initial temperature) to 371 °C, the equilibrium temperature under 1 MPa, can be observed throughout the H_2 storage media at 10 minutes (Fig. 5(a)). The released heat of reaction is

transferred towards the $Mg(OH)_2$ material where it is stored, and its temperature starts to rise, especially at the interface between the two storage media. However, it takes more than 140 minutes to observe the start of the MgH_2 bed cooling, and a uniform temperature distribution throughout the thermochemical heat storage media indicating that the reaction is completed. This is mainly due to the low thermal conductivity of the $Mg(OH)_2$ material which is approximatively eighteen times lower than the one of the hydride bed (Compare their values in Table 1).

Fig. 5(b) illustrates how the reacted fractions of hydrogen and water vapor evolve over time. From t = 10 min to t = 140 min, it is clear that the H_2 absorption and dehydration fronts move into opposite directions. In the hydride zone, a saturation area where the hydride bed is fully charged in hydrogen (x_{abs} = 1) is observed close to the interface separating the two storage materials due to the decrease of the hydride temperature, whereas no hydrogen storage occurs at the central region as a result of the high equilibrium temperature imposed by the H_2 absorption pressure. As time proceeds, the saturation area expands with a very sharp zone towards the central region of MgH_2 bed. In the thermochemical heat storage material zone, the dehydration reaction (see Eq. (2)) is promoted first at the interface (y_{dehy}= 0) due to the exchange of the heat of H_2 absorption reaction. Thereafter, a broad annular zone where magnesium oxide (MgO) is formed moves towards the external wall of the combination reactor. At t = 150 min, all the hydride bed is fully loaded in hydrogen, while the dehydration reaction continues to proceed at a slow rate in the external annular region of the thermochemical heat storage media because of the inefficient heat transfer to this area.

4.2. Temperature and reacted fractions analysis

In order to have a better insight into the thermal interaction of the hydrogen and thermochemical heat storage media, the temporal evolutions of their temperature and reacted fractions at selected indicated locations are presented in Figs. 6(a), (b) and 7(a), (b).

Fig. 6(a) shows a sharp increase of the MgH_2 bed temperature at locations P_1, P_2 and P_3 separated by one fourth of the MgH_2 bed thickness, a few minutes after the start of hydrogen uptake. Thereafter, a horizontal plateau where the temperature is maintained equal to the equilibrium one (371 °C at 1 MPa) is observed. Its length is longer at locations more distant from the interface $MgH_2/Mg(OH)_2$, since the rate of heat transfer towards the thermochemical heat storage media is slower. The equilibrium temperature of 371 °C represents the maximum to be reached by the MgH_2 media, and implies that the H_2 pressure and the equilibrium pressure are equal. Thus, there is no driving potential for hydrogen uptake (see Eqs. (3) and (4)), and the reaction is stopped as it can be seen from Fig. 6(b) where the H_2 absorption fraction, x_{abs} stabilizes at less than 0.1, especially at locations P_2 and P_1. Due to the cessation of the H_2 absorption reaction, there is no more release of the heat of absorption reaction, and the heat already generated is transferred towards the $Mg(OH)_2$ media by conduction at a very slow rate due the low thermal conductivity of the thermochemical heat storage media. As soon as a small decrease of the MgH_2 bed temperature is observed (a few degree Celsius), the driving potential for H_2 absorption increases again, and the related reaction is reactivated. Thus, the H_2 absorption fraction rises sharply towards saturation (x_{abs} = 1) as illustrated in Fig. 6(b). By comparing

locations P_3 and P_1, for example, it can be seen that the time required to the completion of the H_2 absorption reaction in the latter case (152 min) is almost two times longer than the one required at location, P_3 (70 min) due to the limited heat transfer rate towards the $Mg(OH)_2$ media. With the completion of H_2 uptake at the three selected locations, their temperature profiles overlap while decreasing rapidly towards 300 °C, the initial temperature of the MgH_2-$Mg(OH)_2$ combination reactor.

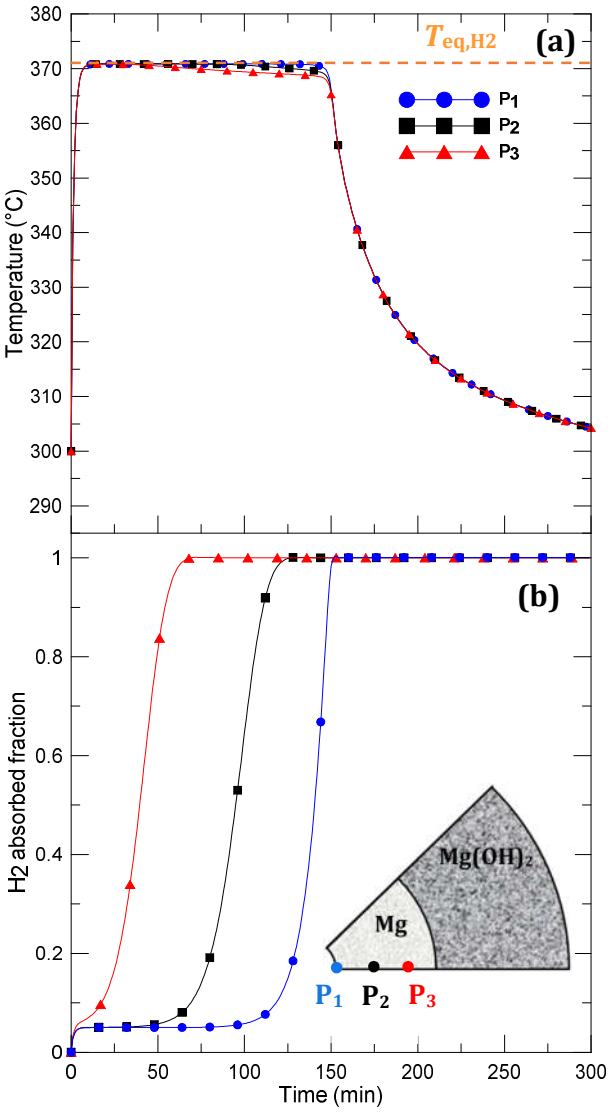

Fig. 6. Time evolution of the (a) temperature and (b) H_2 absorption fraction at three locations of the MgH_2 bed.

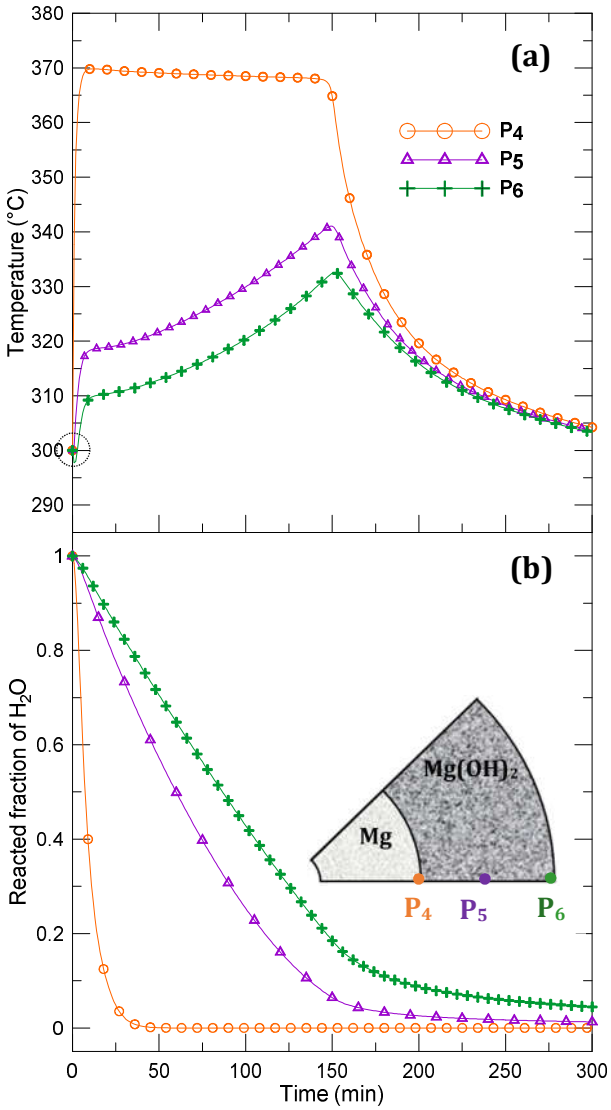

Fig. 7. Time evolution of the (a) temperature and (b) H_2O reacted fraction at three locations of the $Mg(OH)_2$ bed.

Fig. 7(a) shows the temporal evolution of the temperature at three selected locations of the heat storage media (P_4, P_5 and P_6), separated by one half of its thickness. It is worth noting that although an immediate increase of the temperature is observed at locations P_4 and P_5, P_6 which is the farthest away from the interface $MgH_2/Mg(OH)_2$ experiences a slight temperature decrease, which is below 300 °C the initial temperature of the combination reactor (Dashed circle in Fig. 7(a)). This shows that even at location P_6 where there is no heat transfer from the MgH_2 media yet, the endothermic dehydration reaction is initiated at a very early stage. After a sharp increase of the temperature at the three locations due to the storage of heat generated by the absorption of hydrogen in the hydride bed, location P_4 starts to be cooled, following the same trend as observed in the MgH_2 media; whereas the temperature at locations P_5 and P_6 continues its rise at a slower rate compared to the first 10 minutes of the dehydration reaction until it reaches a maximum at t = 150 min. From

that moment, the temperature at the three selected locations drops back to 300 °C, the initial temperature of the combination reactor, after 300 minutes of simulation. The peak of temperature observed at t = 150 min coincides with the one observed in Fig. 6(a), and showing that the H_2 uptake is completed throughout the hydride bed, implying that no more heat generated by the hydrogen absorption reaction is available to be stored by the dehydration reaction. This is confirmed by the temporal evolution of the reacted fraction of water vapor illustrated in Fig. 7(b).

Indeed, apart from location P_4 where the dehydration of $Mg(OH)_2$ is almost completed (y_{dehy} = 0) after about 25 minutes due to the fast heat exchange with the MgH_2 media, the dehydration reaction advanced at a reasonable rate at locations P_5 and P_6 during the first 150 min, then it slows down once no more heat is released by the hydride bed, and it is not even completed after 300 minutes of simulation. In addition, location P_5 experiences a faster decrease of its dehydration rate compared to location P_6 situated at the external wall of the adiabatic combination reactor. This shows that the low thermal conductivity of the thermochemical material is the limiting step of heat exchange between the MgH_2 and $Mg(OH)_2$ beds.

4.3. Hydrogen absorption time and thermal performance of the MgH_2-$Mg(OH)_2$ combination reactor

As stated earlier, the geometric characteristics of the MgH_2-$Mg(OH)_2$ combination reactor modeled herein were chosen identical to the ones used in [17], in order to compare the H_2 absorption time predicted numerically to the one calculated based on the analytical study. Fig. 8(a), (b) shows the profiles of the average temperature and reacted fraction for the hydrogen and thermochemical heat storage media, respectively. It can be seen from Fig. 8(a) that the MgH_2 bed is fully loaded in hydrogen after **150 minutes** (x_{abs} = 1). In the same interval of time, only 92% of water vapor is released by the thermochemical heat storage media (y_{dehy}= 0.08), and the dehydration reaction continues to take place at a very slow rate for the rest of the simulation time while the temperature decreases to 300 °C (see Fig. 8(b)).

Compared to the analytical study results [17], for a $Mg(OH)_2$ bed with a radius of 3.78 cm, it was found that it takes **180 minutes** to fully load the hydride bed in hydrogen, which is 30 minutes longer than the H_2 absorption time predicted numerically. However, by recalling that the analytical study was conducted while assuming constant temperatures of the hydrogen and thermochemical heat storage media of 370 and 340 °C, respectively, this could explain the reason for achieving a faster H_2 loading process when modeling the thermal behavior of the MgH_2-$Mg(OH)_2$ combination reactor. Indeed, the value of the $Mg(OH)_2$ bed temperature used in the analytical analysis was chosen constant, and equal to the PCM melting temperature of the MgH_2-PCM tank developed by Garrier et al. [13]; whereas in the case of the MgH_2-$Mg(OH)_2$ combination reactor, the temperature of the thermochemical heat storage media is variable, and it ranges from 321 °C after 7 minutes of the start of the dehydration reaction to 342°C after 150 minutes, as it can be seen from Fig. 8(b). This corresponds to an average temperature of the thermochemical heat storage media of about 331.5 °C, which is 8.5 °C lower than the PCM melting temperature, and thus justifies the difference between the H_2 absorption times determined analytically and numerically. The numerical results also confirm that the assumption made in the analytical

study, stating that the kinetics of the H_2 absorption and dehydration reactions are not the limiting steps for the two studied materials is also valid.

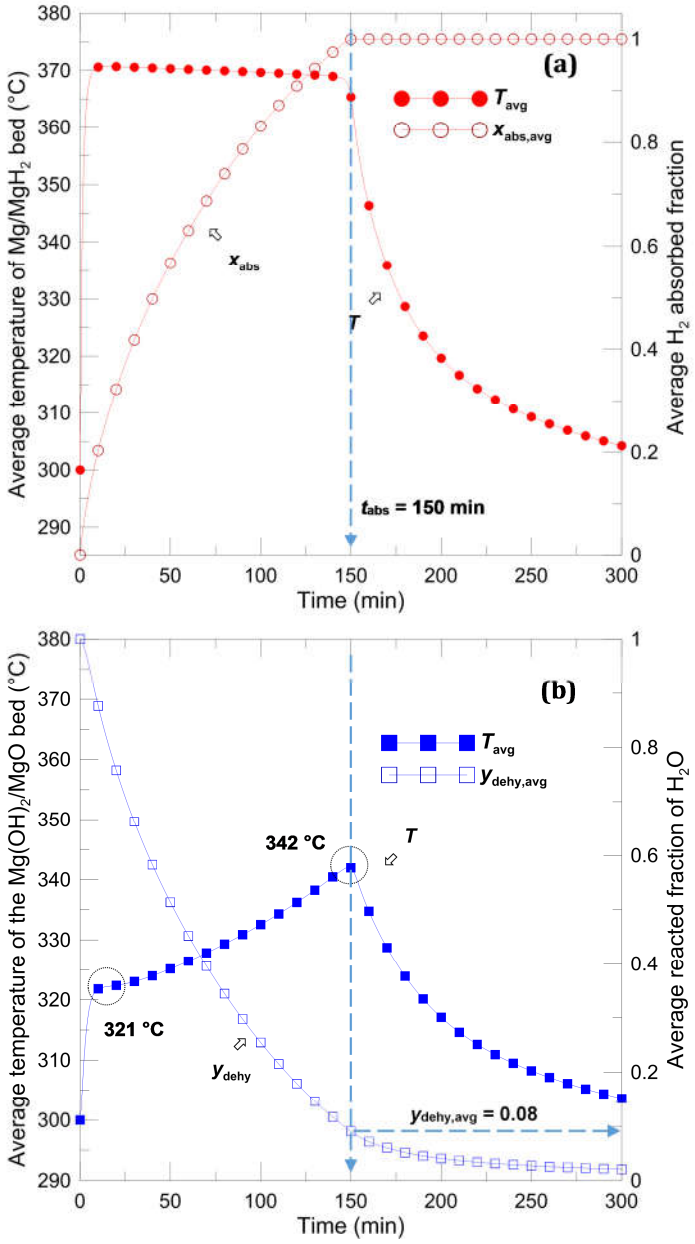

Fig. 8. Time evolution of the average temperature and reacted fraction (a) of the MgH_2 bed and (b) the $Mg(OH)_2$ bed.

The dehydration of the thermochemical material, $Mg(OH)_2$ is an endothermic reaction where the required heat to be stored corresponds to the one generated during the hydrogen uptake in the magnesium hydride bed. The amount of heat exchanged between the MgH_2 and $Mg(OH)_2$ beds can be determined based on the following expressions:

$$Q_{\text{abs}} = \frac{w_t \cdot \rho_{\text{MgH}_2} \cdot (1-\varepsilon) \cdot \pi \cdot (R_2^2 - R_1^2) \cdot \Delta H_{\text{abs}}}{\text{M}_{\text{H}_2}} \quad (16)$$

$$Q_{\text{dehy}} = \frac{\Delta y_{\text{dehy}} \cdot \rho_{\text{Mg(OH)}_2} \cdot \phi \cdot \pi \cdot (R_3^2 - R_2^2) \cdot \Delta H_{\text{dehy}}}{\text{M}_{\text{Mg(OH)}_2}} \quad (17)$$

Using the properties of MgH_2 and $Mg(OH)_2$ materials summarized in Table 1, Q_{abs} and Q_{dehy} are calculated, and compared to the ones determined numerically by taking the integrals versus time of $\dot{Q}_{abs}$ (Eq. (8)) and $|\dot{Q}_{\text{dehy}}|$ (Eq. (9)) plotted in Fig. 9. The obtained results are summarized in Table 2.

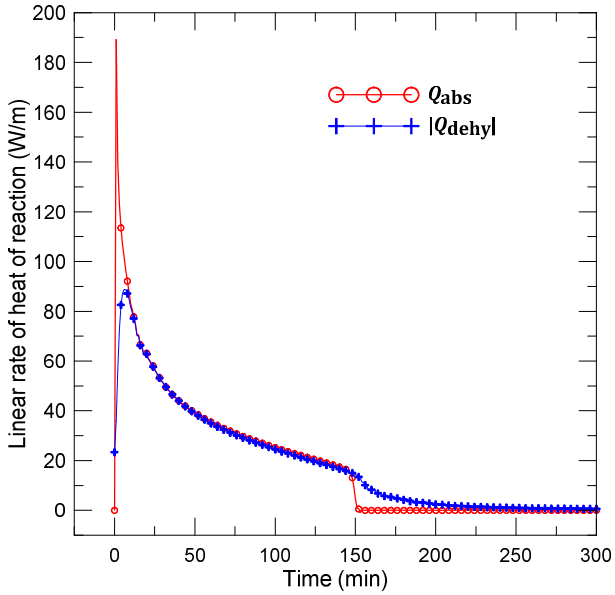

Fig. 9. Time evolution of the linear heat generation and consumption rates ($\dot{Q}_{abs}$ and $|\dot{Q}_{\text{dehy}}|$) for the H_2 absorption reaction and the H_2O dehydration reaction, respectively.

Table 2. Comparison of the amounts of heat exchanged between the hydrogen and heat storage media.

Heat of Reaction	(kJ/m)
$Q_{\text{abs},\boldsymbol{Cal}} = Q_{\text{dehy},\boldsymbol{Cal}}$	2857.14
$Q_{\text{abs},\boldsymbol{Num}}$	2807.33
$\lvert Q_{\text{dehy},\boldsymbol{Num}} \rvert$	2799.41

Fig. 9 shows a peak of heat generation rate at the beginning of the absorption of hydrogen ($t < 25$ min), then it drops down as soon as the magnesium hydride bed reaches its equilibrium temperature, as it can be seen from Fig. 8(a). At the same interval of time, the heat transfer towards the thermochemical storage media occurs at a slower rate as a result of its poor thermal conductivity, and a lower peak of heat consumption is observed. After 150 minutes, the H_2 absorption reaction is completed, whereas the heat is still consumed by the thermochemical material leading to the continuing temperature decrease.

By comparing the calculated and numerical values of Q_{abs} and Q_{dehy} presented in Table 2, it can be seen that $Q_{\text{abs},\boldsymbol{Num}}$ and $\left|Q_{\text{dehy},\boldsymbol{Num}}\right|$ are slightly smaller than the ones calculated based on Eqs. (16) and (17). Such small differences of less than 2% can be attributed to some errors in the numerical calculations. Therefore, it can be concluded that, overall, the numerical results describe reliably the thermal behavior of the MgH_2-$Mg(OH)_2$ combination reactor.

4.4. Effect of H_2 absorption pressure

Simulations were performed for different hydrogen absorption pressures, P_{abs} ranging from 0.8 MPa to 1.4 MPa, and the resulting temporal evolutions of the average temperatures and reacted fractions of the hydrogen and thermochemical heat storage media are presented in Fig. 10(a), (b).

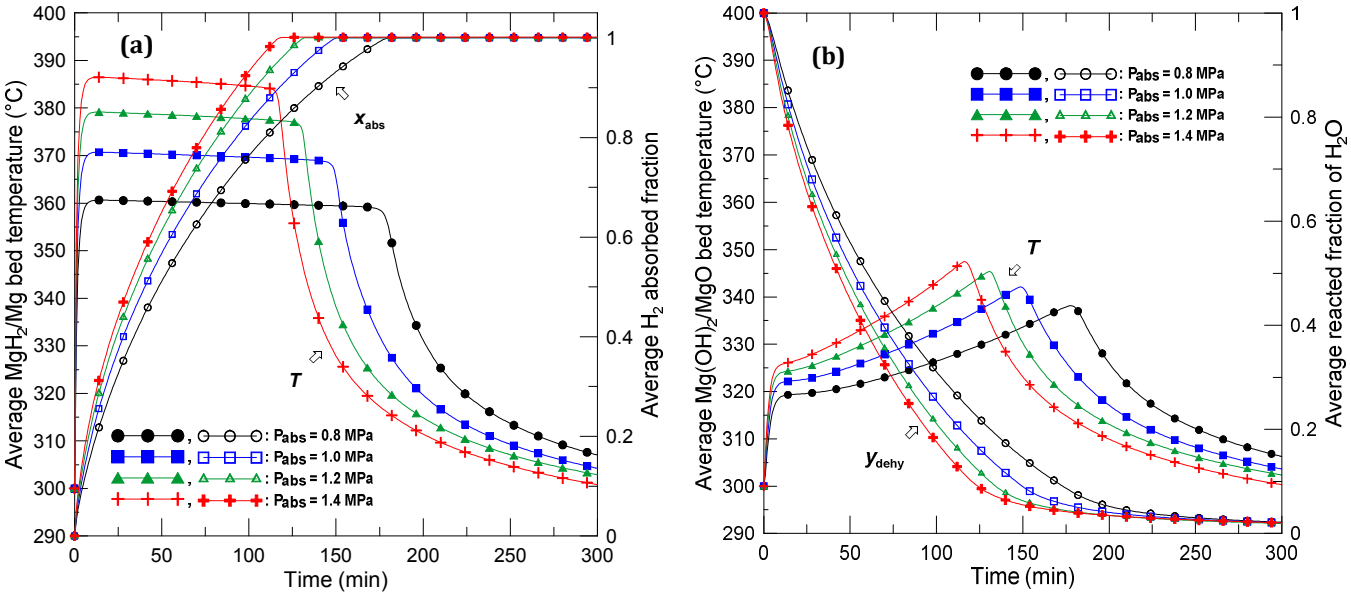

Fig. 10. Effect of the H_2 absorption pressure on the dynamic behavior of the MgH_2-$Mg(OH)_2$ combination reactor: (a) profiles of the average temperature and H_2 absorption fraction of the MgH_2 bed and (b) profiles of the average temperature and H_2O reacted fraction of the $Mg(OH)_2$ bed.

From Fig. 10(a), it can be seen that at the beginning of the H_2 absorption reaction, a sharp increase of the MgH_2 bed temperature is observed regardless the applied hydrogen pressure, thereafter a plateau corresponding to the equilibrium temperature of the H_2 absorption reaction is reached. A higher hydrogen pressure results in a higher equilibrium temperature, and thus a larger temperature gradient between the hydrogen and the thermochemical heat storage media, which promotes a faster heat transfer rate from the MgH_2 bed to the thermochemical material, and a faster reaction rate of the endothermic dehydration reaction as can be seen from Fig. 10(b). As a result, the cooling of the MgH_2 bed also occurs at a faster rate, which ensures a higher driving force of the absorption reaction, and it takes a shorter time to fully load the MgH_2 bed in hydrogen. For instance, comparing the cases where P_{abs} = 1 MPa and 1.4 MPa, shows that the H_2 absorption time in the latter case is about half an hour shorter (see Fig. 10(a)). Therefore, with such a concept

of the MgH_2-$Mg(OH)_2$ combination reactor, the temperature gradients between the hydride and hydroxide media, and thus the H_2 absorption time can be varied by simply imposing different H_2 absorption pressures. This significantly enhances the operation flexibility of such a combination H_2 storage system.

4.5. Effect of the thermal conductivity of the thermochemical heat storage material

For all the results presented above, the thermochemical heat storage media was assumed to be in a pelletized shape of magnesium hydroxide and expanded graphite mixture, with a mass ratio ψ of 8, called EM8 [28]. Despite the addition of the expanded graphite and the packing of the mixture, the obtained thermal conductivity does not exceed the value of 0.55 W/(m.K), which is very low compared to the one of the MgH_2 pellets (see Table 1). Kato et al. [25] showed that a value of 1.2 W/(m.K) can be achieved if the mixture with the same mass ratio, ψ is compressed into a block with larger dimensions compared to the EM8 pellets. By filling the $Mg(OH)_2$ powder in an aluminum matrix foam [17], a bulk thermal conductivity as high as the one of the MgH_2 pellets can be achieved. However, for the three types of material, different densities, as well as different models of the dehydration kinetics are expected [29]. For the sake of simplicity and in order to keep the geometry parameters constant, the effect of the thermal conductivity of the thermochemical heat storage material on the thermal behavior of the MgH_2-$Mg(OH)_2$ combination reactor was numerically explored while assuming the same density of EM8 pellets (Table 1), and the same dehydration kinetics model given by Eq. (9). Fig. 11 shows the effect of this thermophysical property on the temporal evolutions of the average temperatures and reacted fractions of the hydrogen and thermochemical heat storage media.

Based on the obtained results, it is obvious that the dehydration reaction, and the hydrogen absorption process are limited by the heat transfer through the EM8 pellets. Increasing the thermal conductivity of the thermochemical material results in a faster heat consumption rate by the $Mg(OH)_2$ bed, which is described by a larger peak of its average temperature in a shorter interval of time (Fig. 11(a)). This promotes its endothermic dehydration reaction, and a faster dehydration reaction rate is obtained as it can be seen in Fig. 11(b).

As a result of the faster heat transfer and storage rates occurring through the thermochemical heat storage media, the MgH_2 bed cools down more rapidly (Fig. 11(c)), and a sustainable improvement of the rate of absorbed hydrogen is obtained, as illustrated in Fig. 11(d). Indeed, it is possible to achieve a complete hydrogen absorption process in an interval of time of 90 minutes by increasing the value of the thermal conductivity of $Mg(OH)_2$ to 1.2 W/(m.K), compared to 150 min for $\lambda_{Mg(OH)_2}$ = 0.55 W/(m.K). The H_2 absorption time could even be reduced to a half an hour if $\lambda_{Mg(OH)_2}$ = 11 W/(m.K). With this value, which is comparable to the one of the MgH_2 media, the hydrogen absorption process is no longer limited by the heat transfer through the heat storage media. Indeed, the simulation results for $\lambda_{Mg(OH)_2}$ = 15 W/(m.K) show that the temperature and reacted fractions of hydrogen and water vapor overlap with the ones obtained for $\lambda_{Mg(OH)_2}$ = 11 W/(m.K) (see Fig. 11). Nevertheless, it is important to emphasize that the obtained results should be considered with caution since the change of the thermochemical material density and the dehydration kinetics model were not taken into account during simulations. But,

they still give a good insight how the heat transfer through the thermochemical heat storage media could affect the hydrogen absorption process in the MgH_2-$Mg(OH)_2$ combination reactor.

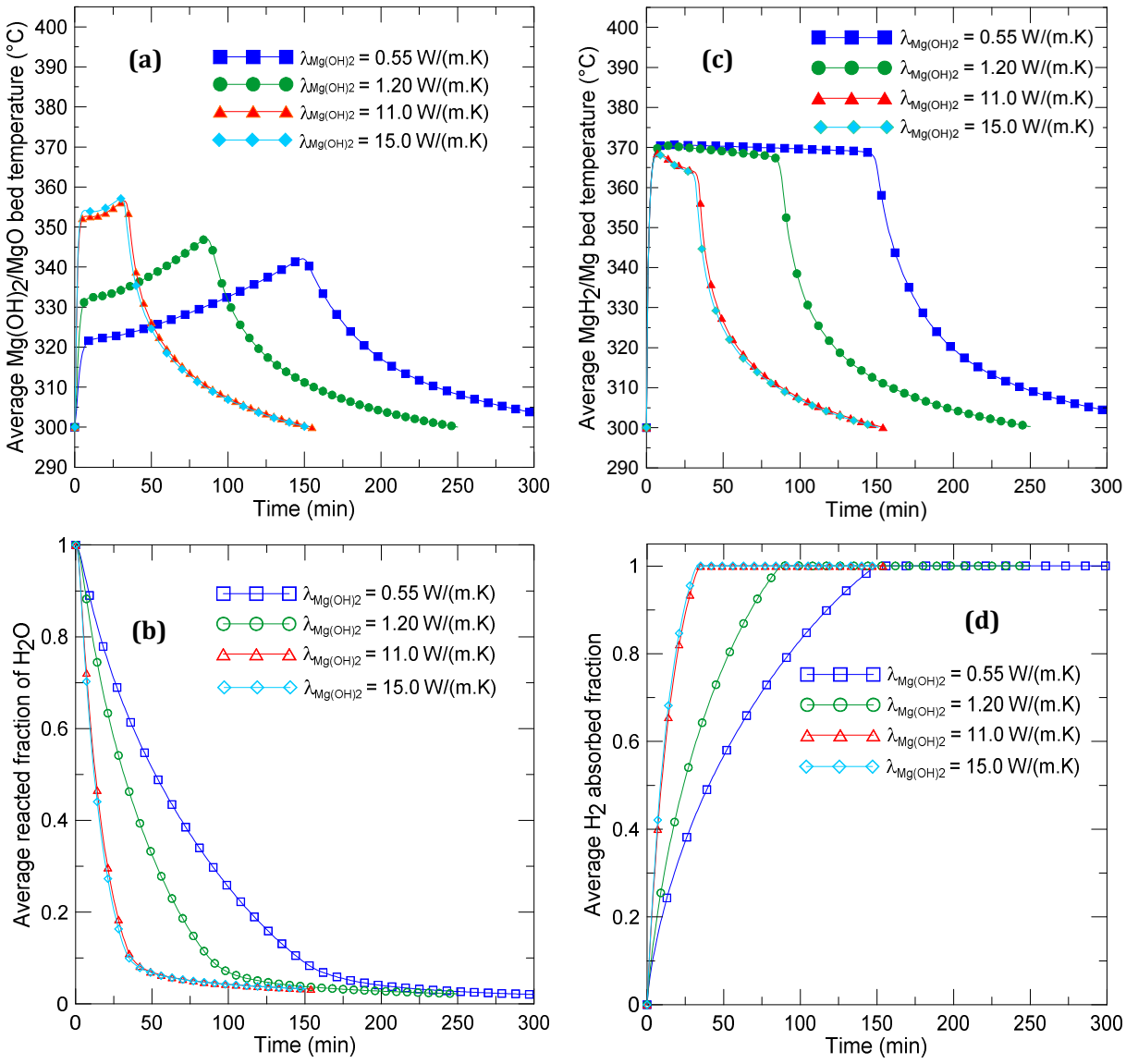

Fig. 11. Effect of the $Mg(OH)_2$ thermal conductivity on the dynamic behavior of the MgH_2-$Mg(OH)_2$ combination reactor: profiles of the average (a) temperature and (b) H_2O reacted fraction of the $Mg(OH)_2$ bed, and profiles of the average (c) temperature and (d) H_2 absorption fraction of the MgH_2 bed.

5. Conclusions

The MgH_2-$Mg(OH)_2$ combination reactor has been demonstrated as a promising technology to store the heat of reaction released during the uptake of hydrogen in order to reuse it in a subsequent hydrogen desorption process. The thermal performance of the proposed

hydrogen storage system has been investigated through the development of a two-dimensional mathematical model describing the simultaneous absorption of hydrogen in the magnesium hydride bed, and the storage of its heat of reaction in the magnesium hydroxide bed. The finite element software, COMSOL Multiphysics was used to solve the coupled equations of kinetics and heat transfer occurring through the two storage media, and the numerical results were validated with experimental data issued from literature. The results obtained from the numerical model have provided a good knowledge of the thermal interaction between the two storage media, and how that would affect the hydrogen absorption time.

- Compared to the results issued from a previous analytical study where the temperature of the $Mg(OH)_2$ bed was set constant and equal to the melting temperature of a PCM material already used in a commercialized PCM-MgH_2 tank, it was found that a larger temperature gradient between the hydrogen and thermochemical heat storage media is achieved, leading to the completion of the hydrogen absorption process in a shorter interval of time.
- The flexibility on the choice of the hydrogen absorption pressure can ensure faster hydrogen absorption rates by generating larger temperature gradients between the MgH_2 and $Mg(OH)_2$ beds.
- By investigating the effect of the $Mg(OH)_2$ thermal conductivity on the thermal performance of the combination reactor, it was found that the heat transfer through the selected type of the $Mg(OH)_2$ material (EM8 pellets) is the limiting step of the hydrogen absorption process. A shorter hydrogen storage time of half an hour could be achieved if the thermal conductivity of the magnesium hydroxide material with a density of 714 kg/m^3 is increased to 11 W/(m.K). Beyond this value, which is comparable to the one of the magnesium hydride pellet, both hydrogen absorption and dehydration reactions are no longer limited by the heat transfer through the thermochemical heat storage media.

Concluding, this study presents first two-dimensional simulation results of an adiabatic hydrogen storage concept based on a thermochemical heat storage material. It presents a suitable mathematical model for two reference materials, and shows the feasibility of the hydrogen absorption process.

References

[1] The Fuel Cell and Hydrogen Annual Review, 2016. 4th Energy Wave, 2016. http://ballard.com/files/PDF/Media/4th_Energy_Wave_2016_FC_and_Hydrogen_Annual.pdf 2016.

[2] McWhorter S, Read C, Ordaz G, Stetson N. Materials-based hydrogen storage: Attributes for near-term, early market PEM fuel cells. Curr Opin Solid State Mater Sci 2011;15:29–38. doi:10.1016/j.cossms.2011.02.001.

[3] Ahluwalia RK, Peng J-K, Hua TQ. Bounding material properties for automotive storage of hydrogen in metal hydrides for low-temperature fuel cells. Int J Hydrogen Energy 2014;39:14874–86. doi:10.1016/j.ijhydene.2014.07.052.

[4] Felderhoff M, Bogdanović B. High temperature metal hydrides as heat storage

materials for solar and related applications. Int J Mol Sci 2009;10:325–44. doi:10.3390/ijms10010325.

[5] Lototskyy M V., Davids MW, Tolj I, Klochko Y V., Sekhar BS, Chidziva S, et al. Metal hydride systems for hydrogen storage and supply for stationary and automotive low temperature PEM fuel cell power modules. Int J Hydrogen Energy 2015;40:11491–7. doi:10.1016/j.ijhydene.2015.01.095.

[6] Corgnale C, Hardy B, Motyka T, Zidan R, Teprovich J, Peters B. Screening analysis of metal hydride based thermal energy storage systems for concentrating solar power plants. Renew Sustain Energy Rev 2014;38:821–33. doi:10.1016/j.rser.2014.07.049.

[7] Srinivasa Murthy S, Anil Kumar E. Advanced Materials For Solid State Hydrogen Storage: "Thermal Engineering Issues." Appl Therm Eng 2014. doi:10.1016/j.applthermaleng.2014.04.020.

[8] Mazzucco A, Dornheim M, Sloth M, Jensen TR, Jensen JO, Rokni M. Bed geometries, fueling strategies and optimization of heat exchanger designs in metal hydride storage systems for automotive applications: A review. Int J Hydrogen Energy 2014;39:17054–74. doi:10.1016/j.ijhydene.2014.08.047.

[9] Bogdanović B, Ritter A, Spliethoff B, Straβburger K. A process steam generator based on the high temperature magnesium hydride/magnesium heat storage system. Int J Hydrogen Energy 1995;20:811–22. doi:10.1016/0360-3199(95)00012-3.

[10] Delhomme B, Lanzini A, Ortigoza-Villalba G a., Nachev S, de Rango P, Santarelli M, et al. Coupling and thermal integration of a solid oxide fuel cell with a magnesium hydride tank. Int J Hydrogen Energy 2013;38:4740–7. doi:10.1016/j.ijhydene.2013.01.140.

[11] Jehan M, Fruchart D. McPhy-Energy's proposal for solid state hydrogen storage materials and systems. J Alloys Compd 2013;580:S343–8. doi:10.1016/j.jallcom.2013.03.266.

[12] Marty P, Rango P De, Delhomme B, Garrier S. Various tools for optimizing large scale magnesium hydride storage. J Alloys Compd 2013;580:S324–8. doi:10.1016/j.jallcom.2013.02.169.

[13] Garrier S, Delhomme B, de Rango P, Marty P, Fruchart D, Miraglia S. A new MgH2 tank concept using a phase-change material to store the heat of reaction. Int J Hydrogen Energy 2013;38:9766–71. doi:10.1016/j.ijhydene.2013.05.026.

[14] Mellouli S, Ben Khedher N, Askri F, Jemni A, Ben Nasrallah S. Numerical analysis of metal hydride tank with phase change material. Appl Therm Eng 2015;90:674–82. doi:10.1016/j.applthermaleng.2015.07.022.

[15] Mellouli S, Abhilash E, Askri F, Ben Nasrallah S. Integration of thermal energy storage unit in a metal hydride hydrogen storage tank. Appl Therm Eng 2016;102:1185–96. doi:10.1016/j.applthermaleng.2016.03.116.

[16] Mellouli S, Askri F, Abhilash E, Ben Nasrallah S. Impact of using a heat transfer fluid pipe in a metal hydride-phase change material tank. Appl Therm Eng 2017;113:554–

65. doi:10.1016/j.applthermaleng.2016.11.065.

[17] Bhouri M, Bürger I, Linder M. Feasibility analysis of a novel solid-state H2 storage reactor concept based on thermochemical heat storage: MgH2 and Mg(OH)2 as reference materials. Int J Hydrogen Energy 2016;41:20549–61. doi:10.1016/j.ijhydene.2016.09.125.

[18] Eugene Long, Boulder; Jeif Schmidt, Superior; Frank Lynch, Conifer all of C. Portable Hydrogen Generator. 5593640, 1997.

[19] Bürger I, Komogowski L, Linder M. Advanced reactor concept for complex hydrides: Hydrogen absorption from room temperature. Int J Hydrogen Energy 2014;39:7030–41. doi:10.1016/j.ijhydene.2014.02.070.

[20] Bürger I, Luetto C, Linder M. Advanced reactor concept for complex hydrides: Hydrogen desorption at fuel cell relevant boundary conditions. Int J Hydrogen Energy 2014;39:7346–55. doi:10.1016/j.ijhydene.2014.02.069.

[21] Bhouri M, Bürger I, Linder M. Optimization of hydrogen charging process parameters for an advanced complex hydride reactor concept. Int J Hydrogen Energy 2014;39:17726–39. doi:10.1016/j.ijhydene.2014.08.100.

[22] Bu I, Bhouri M, Linder M. Considerations on the H2 desorption process for a combination reactor based on metal and complex hydrides 2015:1–11. doi:10.1016/j.ijhydene.2015.03.136.

[23] Visaria M, Mudawar I, Pourpoint T, Kumar S. Study of heat transfer and kinetics parameters influencing the design of heat exchangers for hydrogen storage in high-pressure metal hydrides. Int J Heat Mass Transf 2010;53:2229–39. doi:10.1016/j.ijheatmasstransfer.2009.12.010.

[24] Zamengo M, Ryu J, Kato Y. Magnesium hydroxide – expanded graphite composite pellets for a packed bed reactor chemical heat pump. Appl Therm Eng 2013;61:853–8. doi:10.1016/j.applthermaleng.2013.04.045.

[25] Zamengo M, Ryu J, Kato Y. Composite block of magnesium hydroxide – Expanded graphite for chemical heat storage and heat pump. Appl Therm Eng 2014;69:29–38. doi:10.1016/j.applthermaleng.2014.04.037.

[26] Chaise a., de Rango P, Marty P, Fruchart D. Experimental and numerical study of a magnesium hydride tank. Int J Hydrogen Energy 2010;35:6311–22. doi:10.1016/j.ijhydene.2010.03.057.

[27] Chaise A. Thèse de réservoirs d ' hydrure de magnésium. 2010.

[28] Zamengo M, Ryu J, Kato Y. Thermochemical performance of magnesium hydroxide–expanded graphite pellets for chemical heat pump. Appl Therm Eng 2014;64:339–47. doi:10.1016/j.applthermaleng.2013.12.036.

[29] Zamengo M. A Study on Heat Transfer-Enhanced Composites for a Magnesium Oxide / Water Chemical Heat Pump Author : Massimiliano Zamengo Supervisor : Assoc . Prof ., Dr . Yukitaka Kato Department of Nuclear Engineering. Tokyo Institute of Technology, n.d.

[30] Zamengo M, Ryu J, Kato Y. Numerical Analysis of Chemical Heat Storage Units for Waste Heat Recovery in Steel Making Processes. ISIJ Int 2015;55:473–82. doi:10.2355/isijinternational.55.473.

[31] National Institute of Standards and Technology (NIST). Magnesium hydroxide n.d. http://webbook.nist.gov/cgi/cbook.cgi?ID=C1309428&Type=JANAFS&Table=on.

[32] National Institute of Standards and Technology (NIST). Magnesium oxide n.d. http://webbook.nist.gov/cgi/inchi?ID=C1309484&Type=JANAFS&Plot=on.

[33] POCOGRAPHITE An Entegris Company. Properties and Characteristics of Graphite n.d. http://poco.com/Portals/0/Literature/Semiconductor/IND-109441-0115.pdf.

Nomenclature

Materials

EG: expanded graphite
Mg/MgH_2: magnesium/magnesium hydride
$MgO/Mg(OH)_2$: magnesium oxide/magnesium hydroxide
H_2: hydrogen

Parameters

A: Arrhenius parameter (1/s)
c_p: specific heat capacity (J/(kg.K))
E_a: activation energy (kJ/mol)
m: mass (kg)
M: molecular weight (kg/mol)
P: pressure (MPa)
Q: heat of reaction (kJ or kJ/m)
$\dot{Q}$: volumetric or linear rate of heat of reaction (W/m^3 or W/m)
R: radius (cm)
$\Re$: universal gas constant (J/(mol.K))
t: time (min)
T: temperature (°C)
w_t: Gravimetric H_2 storage capacity (%)
x: absorption fraction (-)
y: dehydration fraction (-)

Greek Letter

ε: porosity (-)
λ: thermal conductivity (W/(m.K))
ρ: mass density (kg/m^3)
ϕ: mixing mass ratio (g of $Mg(OH)_2$:g of (E.G+ $Mg(OH)_2$)
ψ: mixing mass ratio (g of $Mg(OH)_2$:g of E.G)
ΔH: Enthalpy of reaction (kJ/mol)
ΔS: Entropy of reaction (kJ/(K.mol))

Subscripts

abs: absorption
avg: average
dehy: dehydration
eff: effective
eq: equilibrium
ini: initial